

Enzymatic processing of fumiquinazoline F: A Tandem oxidative-
acylation strategy for the generation of multicyclic scaffolds in fungal
indole alkaloid biosynthesis

Brian D. Ames, Xinyu Liu, and Christopher T. Walsh

Department of Biological Chemistry and Molecular Pharmacology

Harvard Medical School, Boston, MA 02115

Supporting Discussion

Characterization of the FQF indoline-2',3'-diol by LC-MS and isotope feeding studies. The MS spectrum of **3** is fairly complex; however, each peak may be accounted for using the structure of **3** as the basis (Figure S8). A peak representing the $[M+H]^+$ ion species is absent from the MS spectrum (from LC-MS/ESI+), though this may be expected as hydroxylation at C2' of **3** generates a hemiaminal functional group susceptible to acid-catalyzed exchange during chromatography and loss as neutral water during ionization. Experimental support that the indole 2'-OH of **3** is derived from water was obtained by using $[^{18}\text{O}]\text{-H}_2\text{O}$ in the reaction setup, resulting in enrichment of the M+2 peaks for the ion species $[2M+\text{Na}]^+$ and $[2M+\text{Na}]^+(-\text{H}_2\text{O})$ compared to a reaction setup using unlabeled water (see lower and middle panel of Figure S8). Of note is that these MS peaks arising from incorporation of the ^{18}O -label of $[^{18}\text{O}]\text{-H}_2\text{O}$ were only observed when acid was omitted from the solvent system used for LC-MS, supporting the lability of the indoline 2'-OH to exchange under acidic conditions.

Figure S1. General structure of the pyrazino[2,1-*b*]quinazoline-3,6-dione ring system and structures of fungal alkaloids discussed in this work that contain this core scaffold.

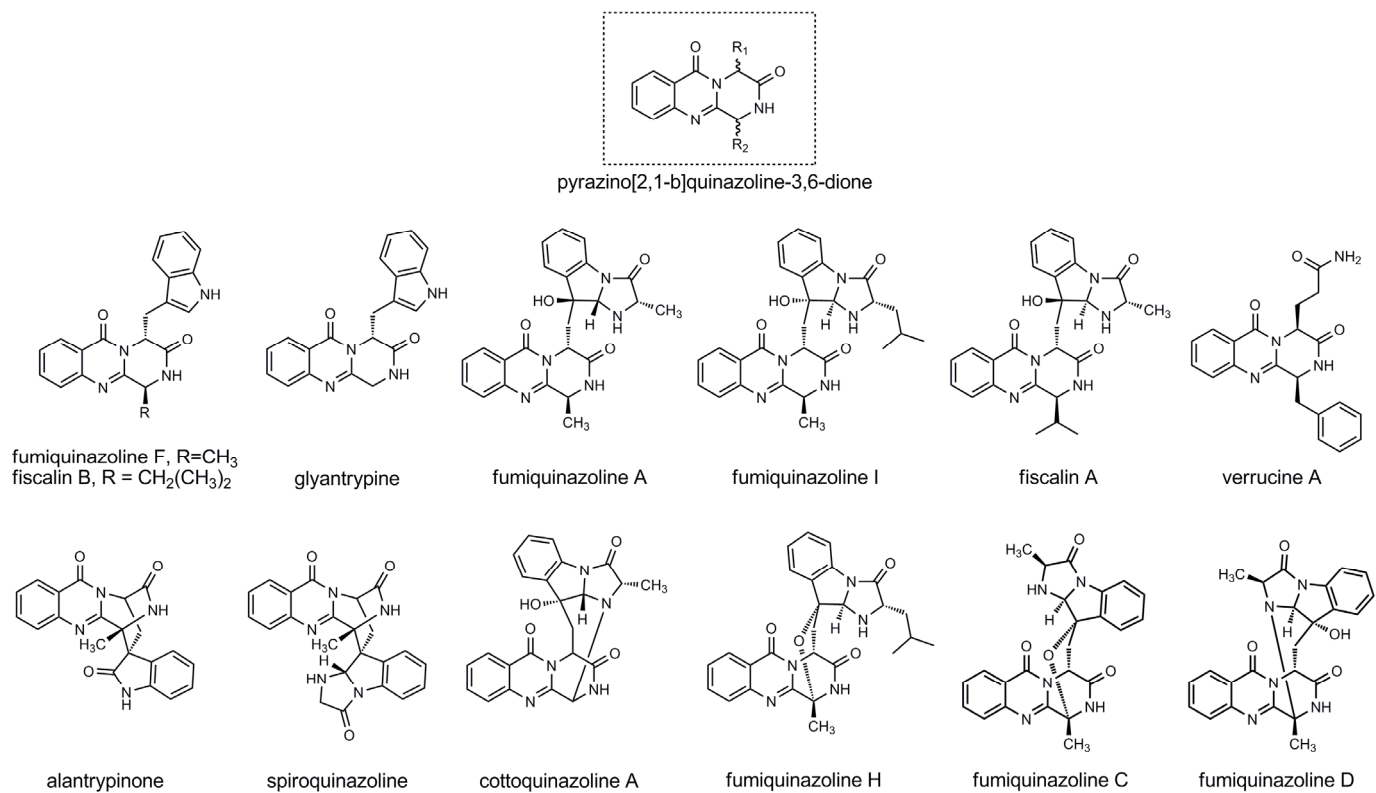
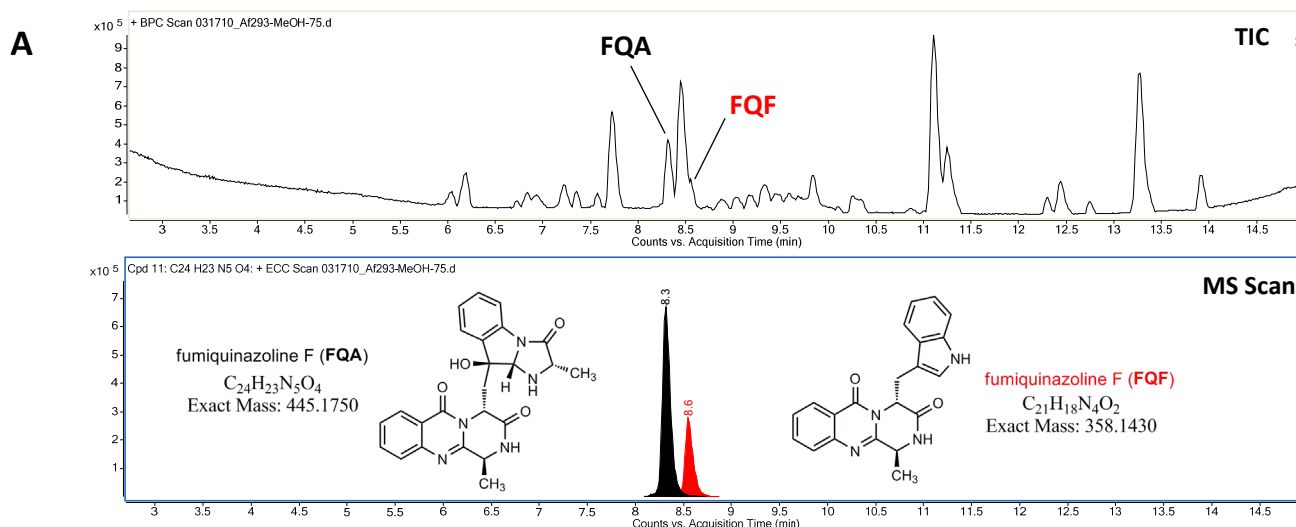


Figure S2. Identification of FQA and FQF from *Aspergillus fumigatus* Af293 culture broth extracts. (A) Base-peak cycled total-ion current (TIC) chromatogram and MS scan of the *A. fumigatus* Af293 extract. The extract was prepared by absorbing 5 mL of clarified culture broth into XAD-16 resin and eluting with 200 μ L MeOH, a 10 μ L volume was injected for analysis. The MS scan shows extracted peaks when filtering for FQA and FQF by formula. Of note is that the large peak between FQA and FQF is not UV-active. (B) High-resolution MS spectra (left); and UV-vis spectra (right), from a separate analytical HPLC run using the same extract) for FQA and FQF.



Ion mass (M+H) ⁺								
Name	RT	Calc.	Target	Diff (ppm)	Formula (Tgt)	Score (Tgt)	Ions	Height
Fumiquinazoline A	8.3	446.1812	446.1823	2.5	$C_{24}H_{23}N_5O_4$	94.1	10	4.2E5
Fumiquinazoline F	8.6	359.1495	359.1503	2.0	$C_{21}H_{18}N_4O_2$	95.5	6	2.1E5

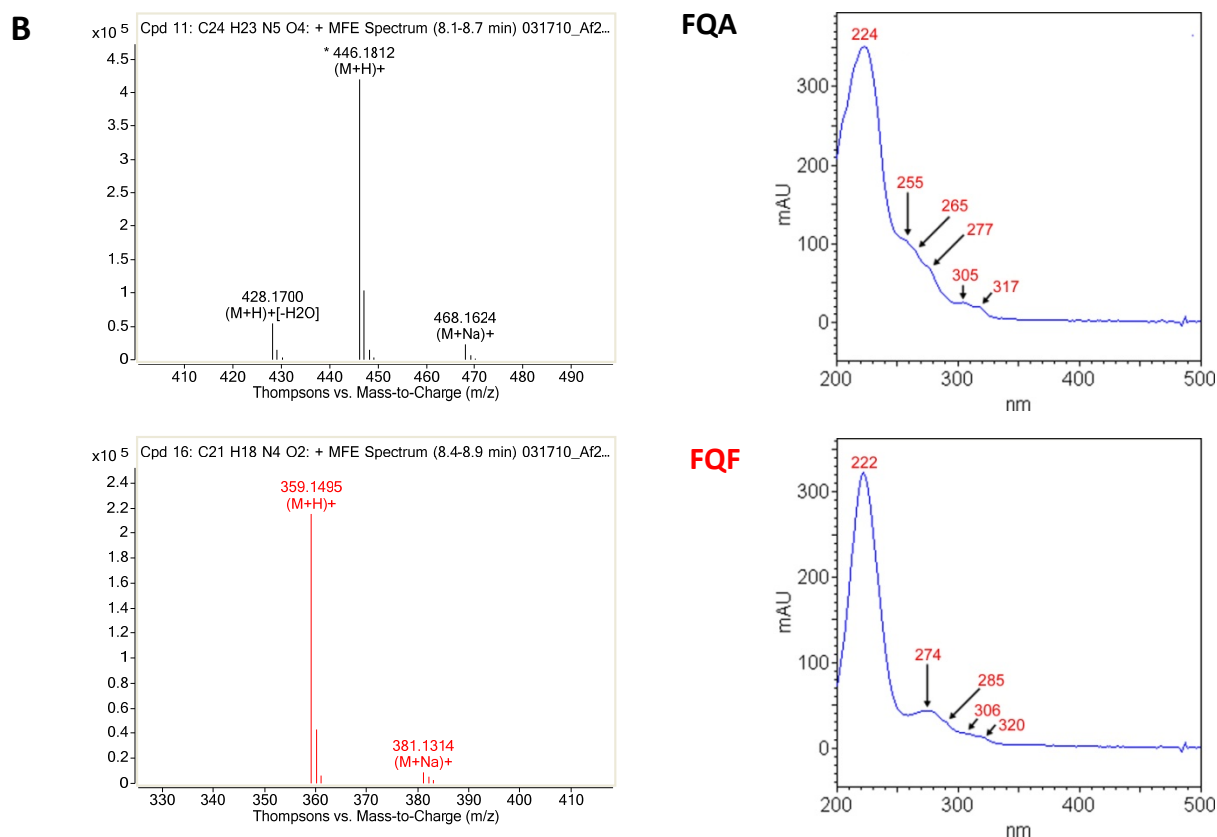


Figure S3. SDS-PAGE gels detailing the purity of Af12060 and Af12050 after expression in *E. coli* and purification of soluble protein by Ni-affinity chromatography. M, marker; E1, elution 1 (5 mL of 250 mM imidazole in buffer).

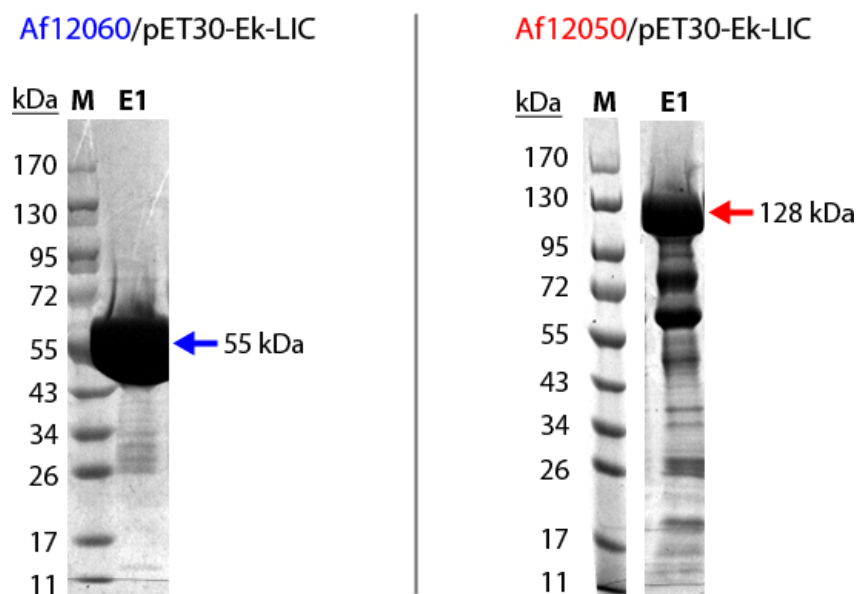


Figure S4. Characterization of Af12060 as an FAD-binding protein. (A) UV-vis spectra (inset, zoom view) of a diluted sample of Ni-NTA purified Af12060 ($\approx 15 \mu\text{M}$) showing peaks characteristic of bound flavin cofactor. $A_{280} = 1.35$, $A_{360} = 0.030$, $A_{450} = 0.038$. Percent holo protein was calculated to be 23% based on $[\text{FAD}]/[\text{Af12060}] \times 100$, using a theoretical extinction coefficient of $91,900 \text{ M}^{-1} \text{ cm}^{-1}$ for Af12060 (at 280_{nm}) and the published extinction coefficient for free FAD of $11,300 \text{ M}^{-1} \text{ cm}^{-1}$ (at 446_{nm})(1). (B) UV-vis spectra of the sample used for (A) following heat-denaturation of the protein (95°C for 10 minutes), and centrifugation to remove precipitate. $A_{260} = 0.32$, $A_{360} = 0.065$, $A_{450} = 0.056$. Calculating percent holo protein based on this data and the A_{280} from (A) yields 34% protein with bound FAD. (C) HPLC trace overlay (260 nm detection) of a $25 \mu\text{L}$ injection of $\approx 140 \mu\text{M}$ Af12060 following heat-denaturation and centrifugation (bottom trace) along with FAD or FMN standards for reference.

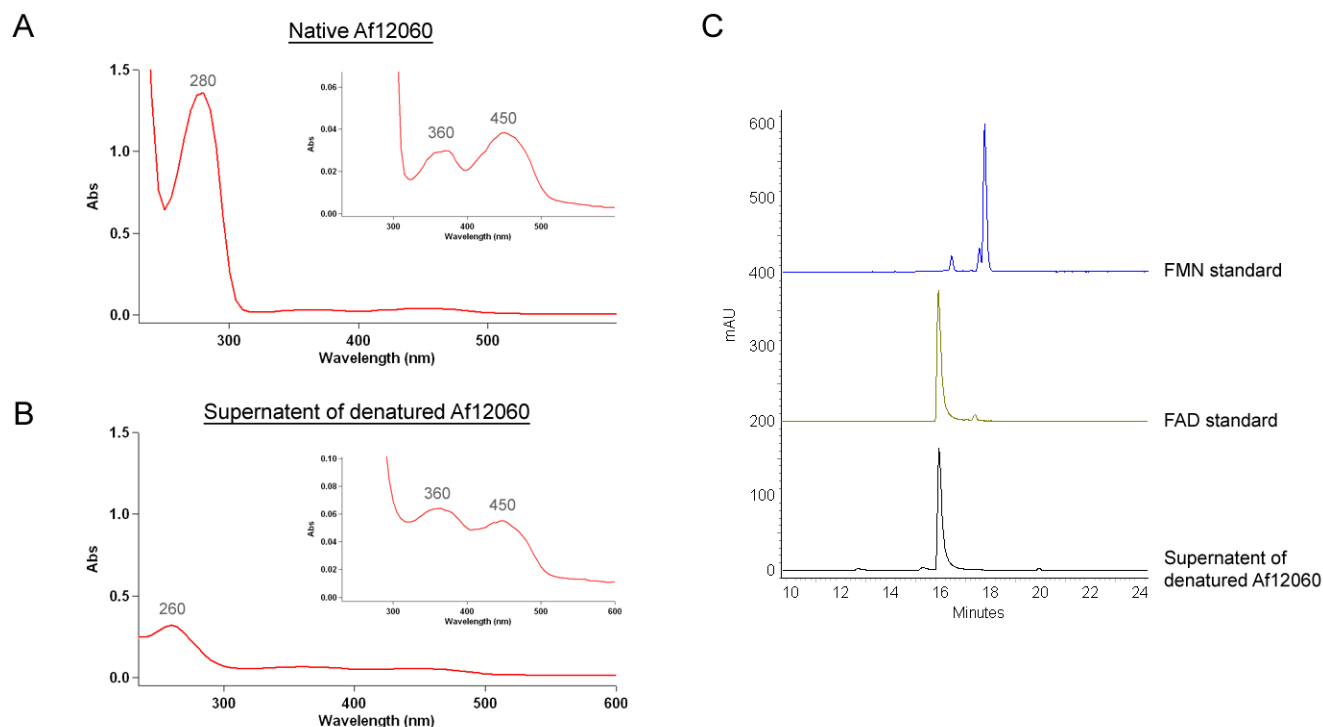
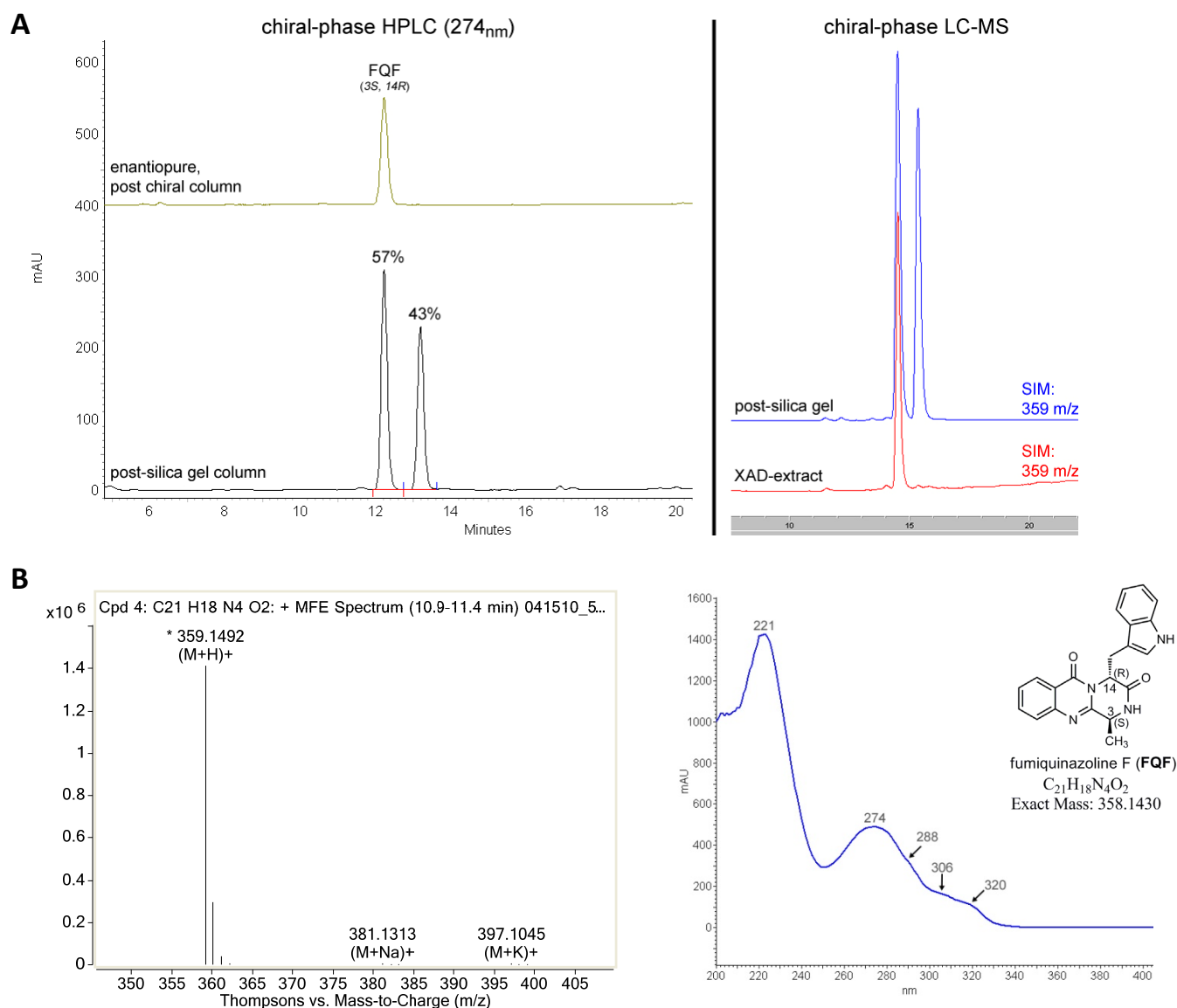


Figure S5. Characterization of the chemically synthesized fumiquinazoline F. (A) Left, chiral-phase HPLC trace of the chemically synthesized FQF post silica-gel flash chromatography (scalemic mixture, 14% ee, bottom trace) and the final enantiopure (3*S*, 14*R*) product. Both traces are derived from detection at 274 nm. Right, chiral-phase LC-MS traces derived from selected ion monitoring (SIM) for the $[M+H]^+$ species of FQF. The top trace represents the scalemic mixture of FQF/enantiomer and is overlaid onto a sample of the biologically-derived FQF from *A. fumigatus* Af293 culture broth (annotated as XAD-extract). (B) High-resolution MS spectrum (left), and UV-Vis spectrum (right) for synthesized FQF.



```
Automation directory: /export/home/bowers/vnmrsys/data/auto_2009.10.26_01
File : exp
Sample id : tmpstudy
```

```

Pulse Sequence: s2pul
Solvent: cdcl3
Temp. 25.0 C / 298.1 K
Operator: bowders
VMRS-600 "nmr"

Relax. delay 1.000 sec
Pulse 45.0 degrees
Acq. time 2.049 sec
Width 9615.4 Hz
25 repetitions
OBSERVE H1, 599.767964 MHz
DATA PROCESSING
line broadening 0.2 Hz
FT size 65336
Total time 1 min, 22 sec

```

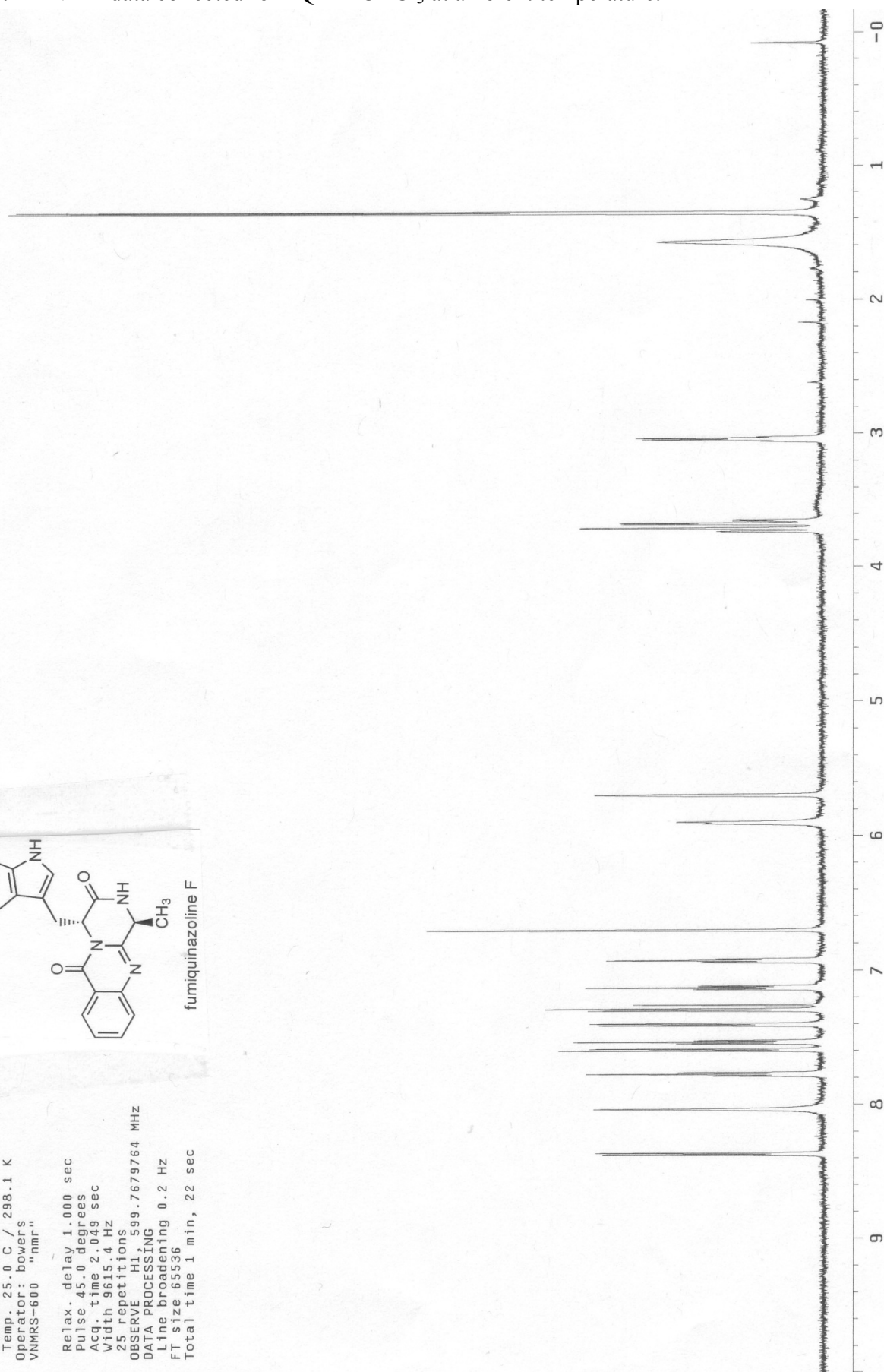
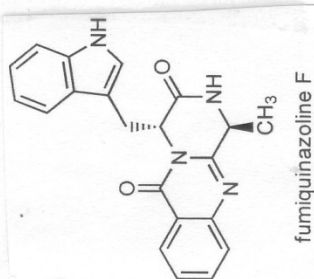


Figure S7. Data from spectrophotometric assay monitoring the consumption of NADPH (decrease in A_{340}) with varying concentrations of FQF as substrate and 1 μM Af12060 +/- 5 μM holo-Af12050. All reactions (200 μL) contained 200 μM NADPH in NaP_i buffer, pH 7.4; when holo-Af12050 was used in combination with Af12060 additional components included 1 mM ATP, 1 mM L-Ala, and 2 mM MgCl_2 . Assays were performed in triplicate for each concentration of FQF tested, and the initial rate data (in A_{340}/min) was converted to the rate of NADPH consumption (in $\mu\text{M}/\text{min}$) using the molar extinction coefficient for NADPH of $6220 \text{ M}^{-1} \text{ cm}^{-1}$. The presence of 5:1 molar excess Af12050:Af12060 did not relieve the concentration-dependent FQF inhibition of NADPH consumption observed when assaying Af12060 alone, supporting substrate and not product inhibition of Af12060.

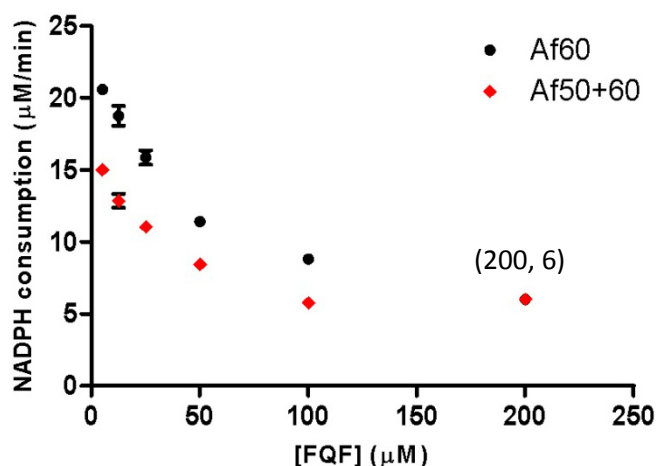
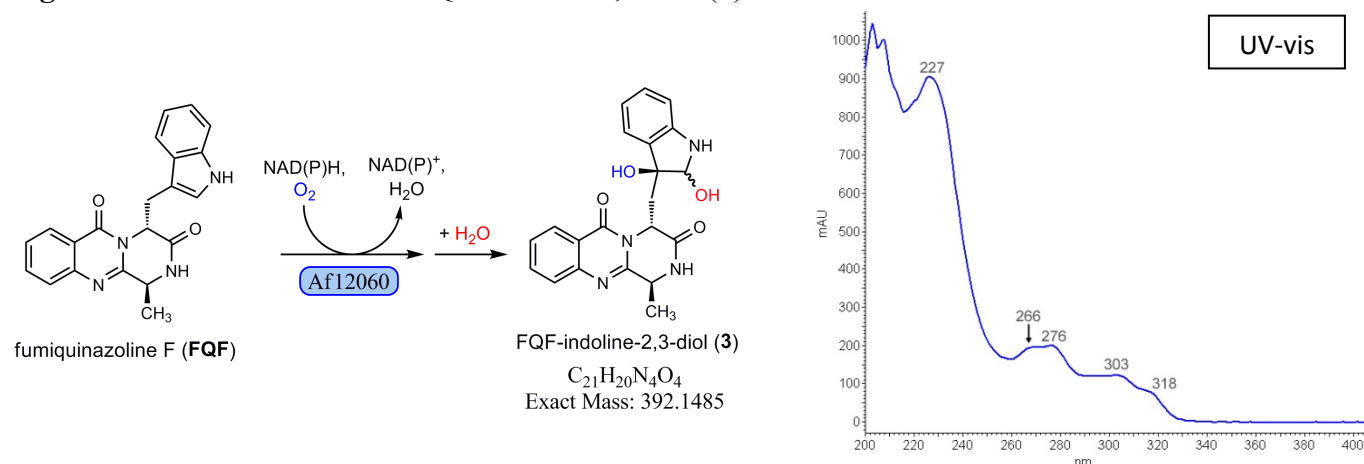
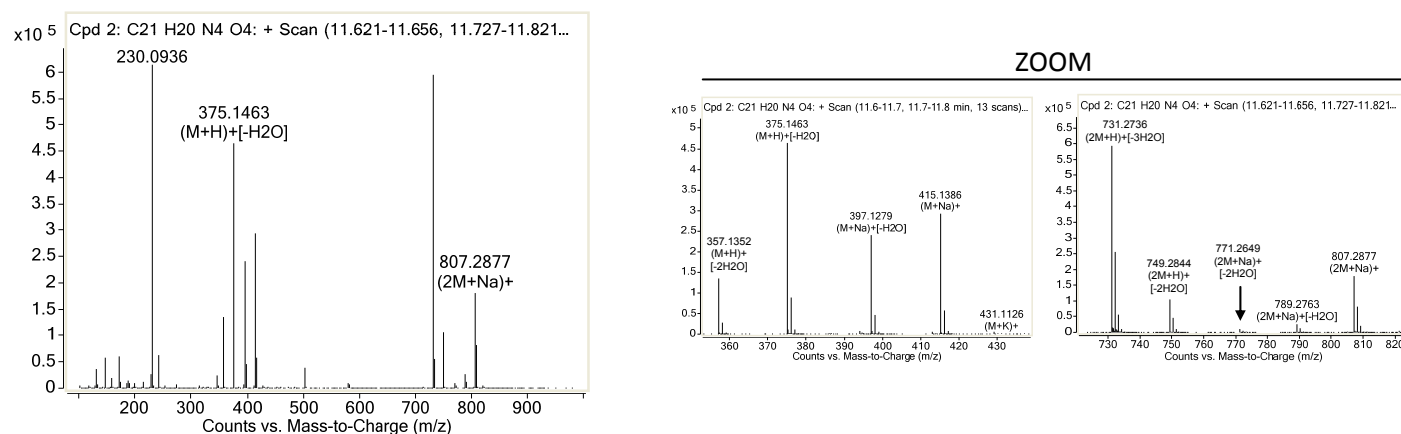


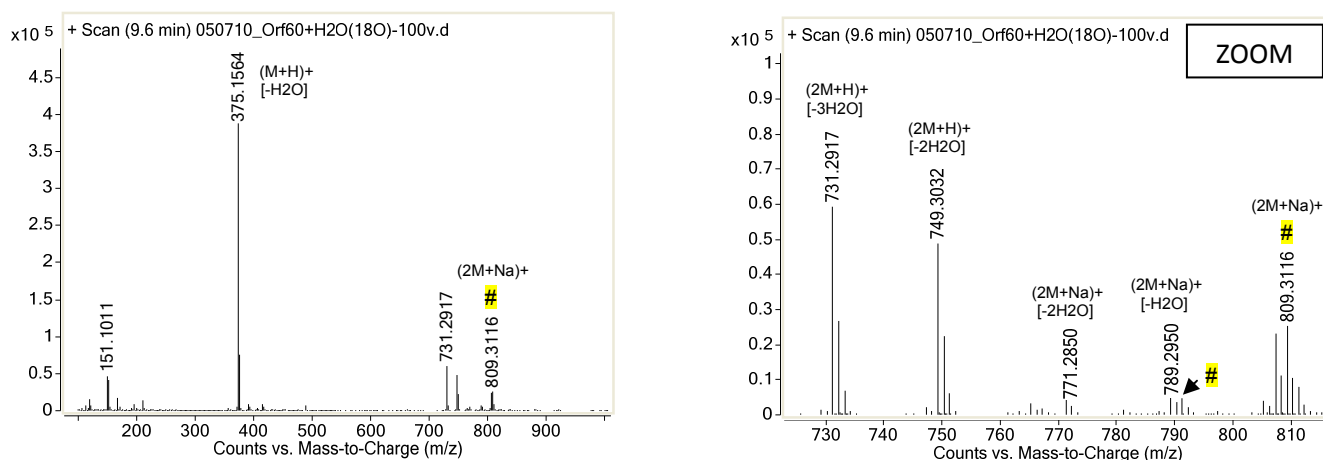
Figure S8. Characterization of FQF-indoline-2,3-diol (**3**).



Mass spectrum of **3** from LC-MS run performed with solvent including 0.1% formic acid:



Mass spectrum of **3** from LC-MS run performed using solvent without acid, [¹⁸O]H₂O used in assay:



denotes peaks with the diagnostic 2Da mass shift indicating incorporation of [¹⁸O]H₂O. The [¹⁸O] label is not present in the peaks at 375, 731, 749, and 771 m/z, indicating that this position is labile to neutral loss of H₂O during ionization. It is also of note that under acidic running LC-MS running conditions (0.1% formic acid), no incorporation of the [¹⁸O] label is observed, most likely due to acid-catalyzed exchange at this position during chromatography.

Figure S9. Characterization of FQF-oxidized dimer (**4**). (A) Four possible structures for **4** (molecular formula: $C_{42}H_{36}N_8O_6$; exact mass: 748.2758). (B) High-resolution MS spectrum (left), and UV-Vis spectrum from separate analytical HPLC run (right).

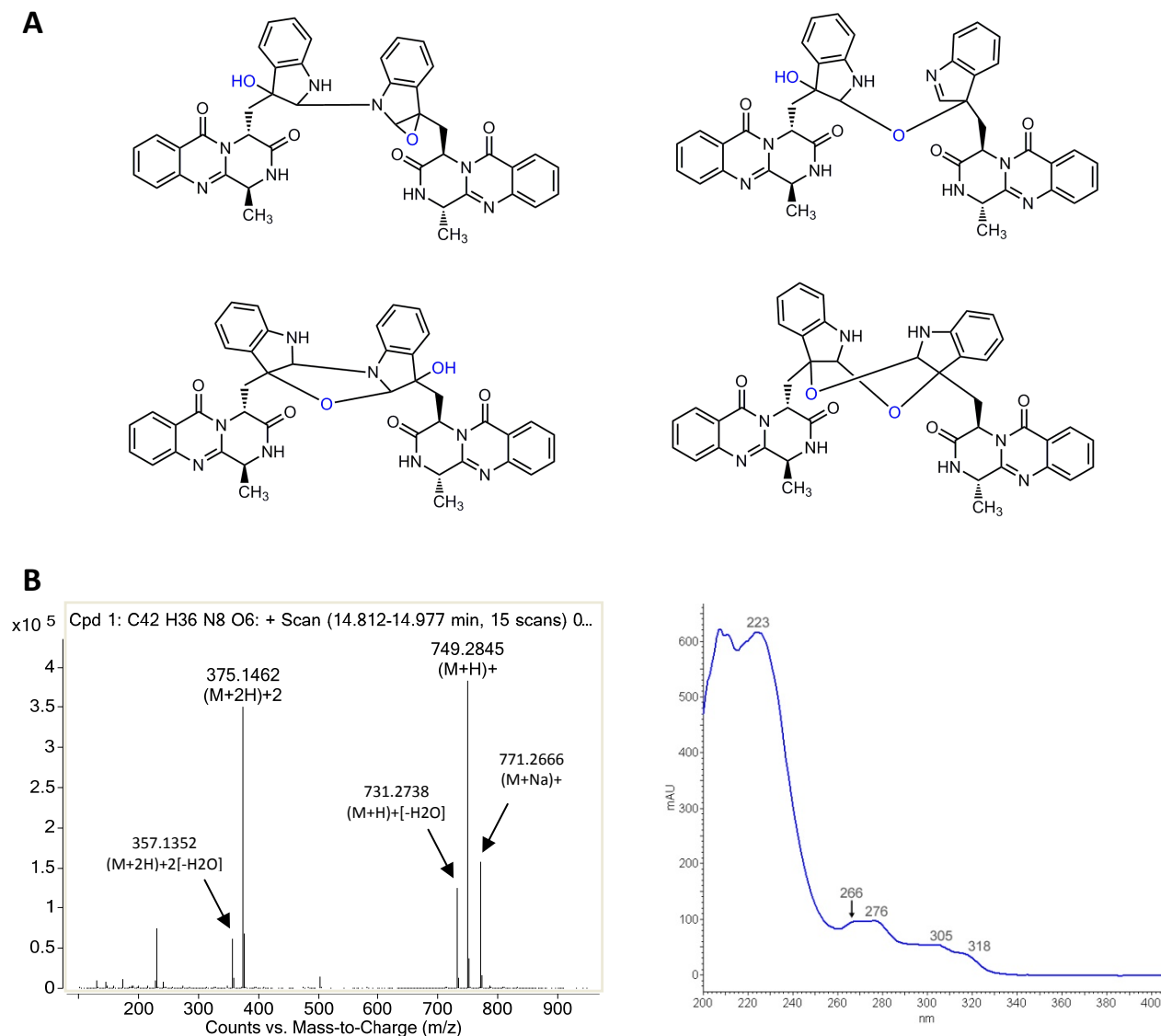


Figure S10. Characterization of the enzymatically synthesized fumiquinazoline A. (A) High-resolution MS spectrum (left), and UV-Vis spectrum (right) of enzymatically prepared FQA. The *in vitro* biosynthesis of FQA was performed by combining FQF, Af12060, holo-Af12050, NADPH, ATP, L-Ala and MgCl₂ in buffer, followed by precipitation of protein and preparative HPLC purification. (B) Left, chiral-phase HPLC characterization (274 nm) of the enzymatically prepared FQA reverse-phase HPLC indicating the enzymatic product is a single enantiomer; right, reverse-phase LC-MS traces derived from selected ion monitoring (SIM) for the [M+H]⁺ species of FQA. The top trace represents the purified FQA and is overlaid onto a sample of the biologically-derived FQA from *A. fumigatus* Af293 culture broth (annotated as XAD-extract).

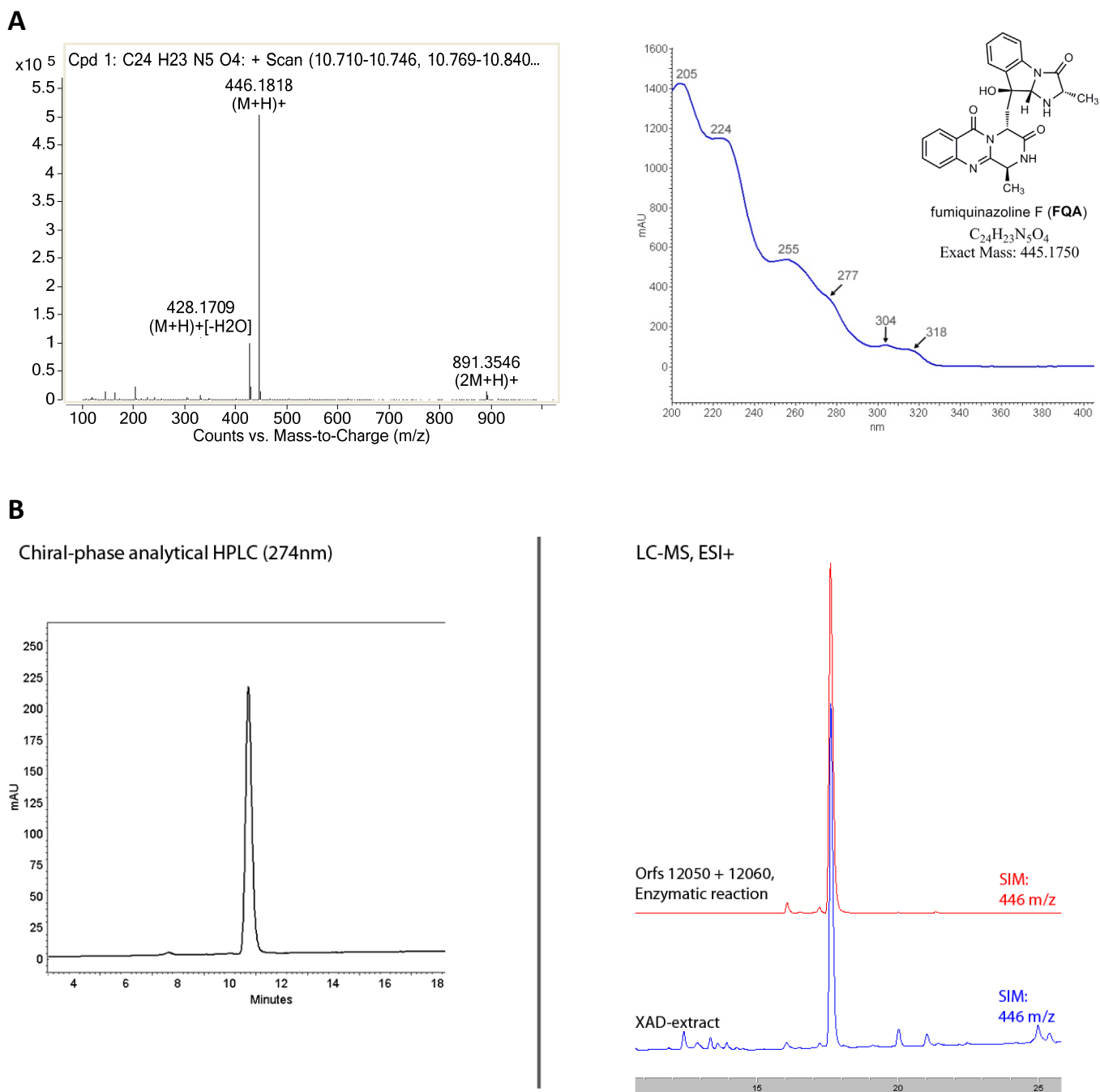


Figure S11. ^1H -NMR data collected for FQA in CDCl_3 at ambient temperature.

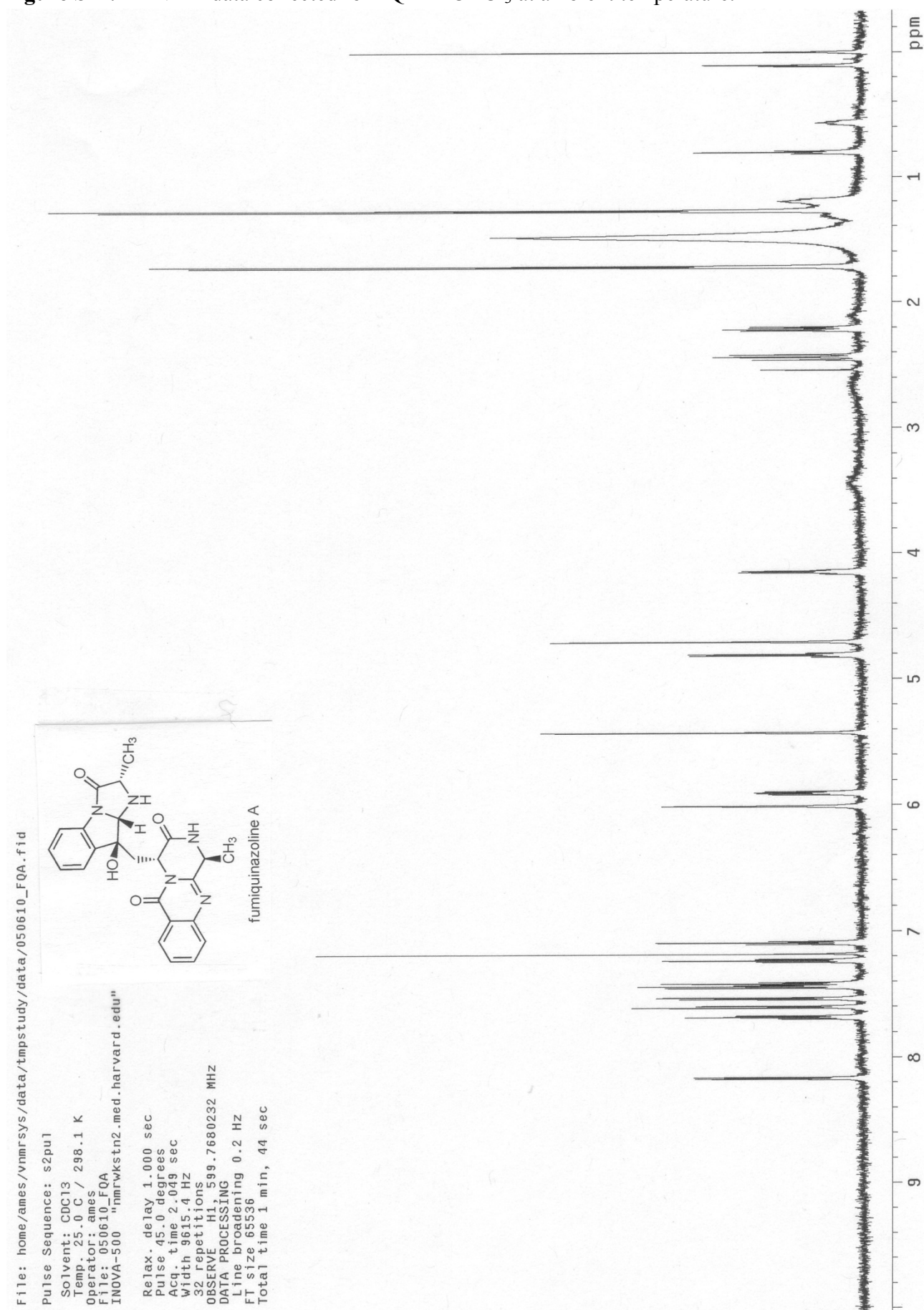


Figure S13. (A) Schematic for the enzymatic conversion of FQF to an FQA analog incorporating glycine to form the imidazolidinolone moiety (**8**). (B) LC-MS trace overlay. The MS scan shows extracted peaks when filtering for **3**, **8**, **FQF**, and **4** by formula. (C) LC-MS spectra (left) and UV-Vis spectra (right) for **8**, and LC-MS spectra for **3**, **FQF**, and **4**. Scalemic FQF was used in assay, therefore the unreacted FQF present is likely the (3*R*, 14*S*) enantiomer.

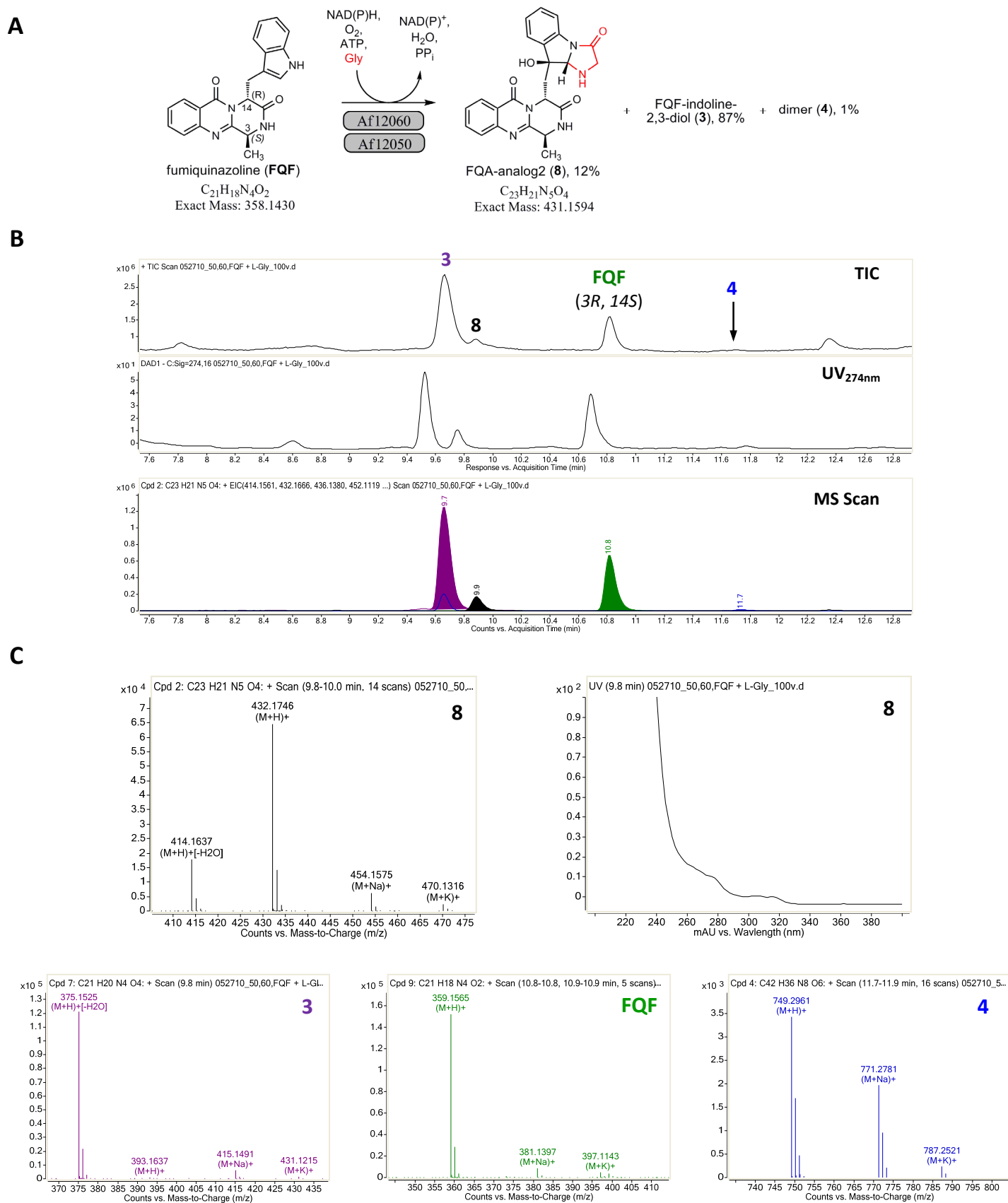


Figure S14. ^1H -NMR data collected for glyantrypine in CDCl_3 at ambient temperature (major contaminants labeled).

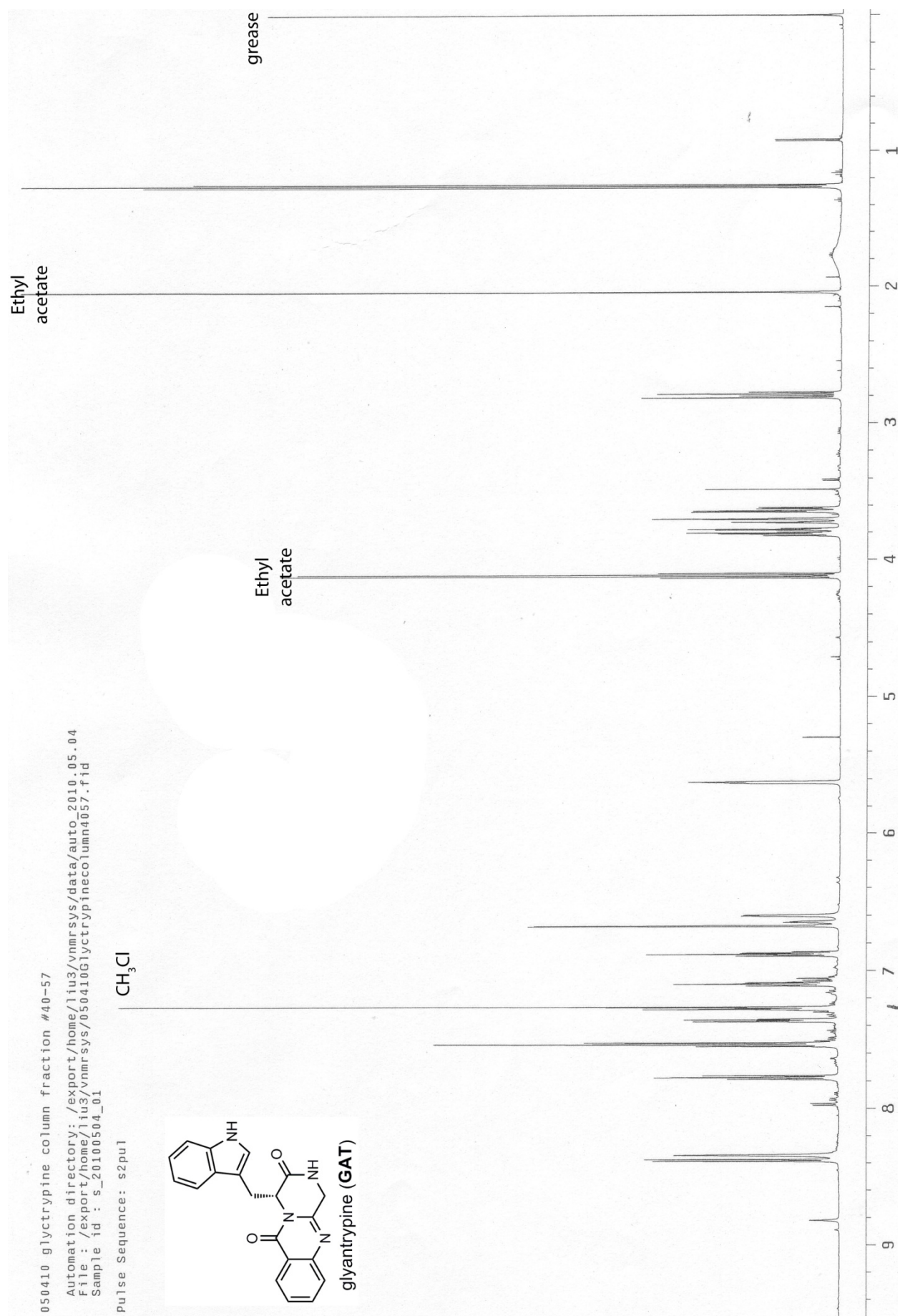
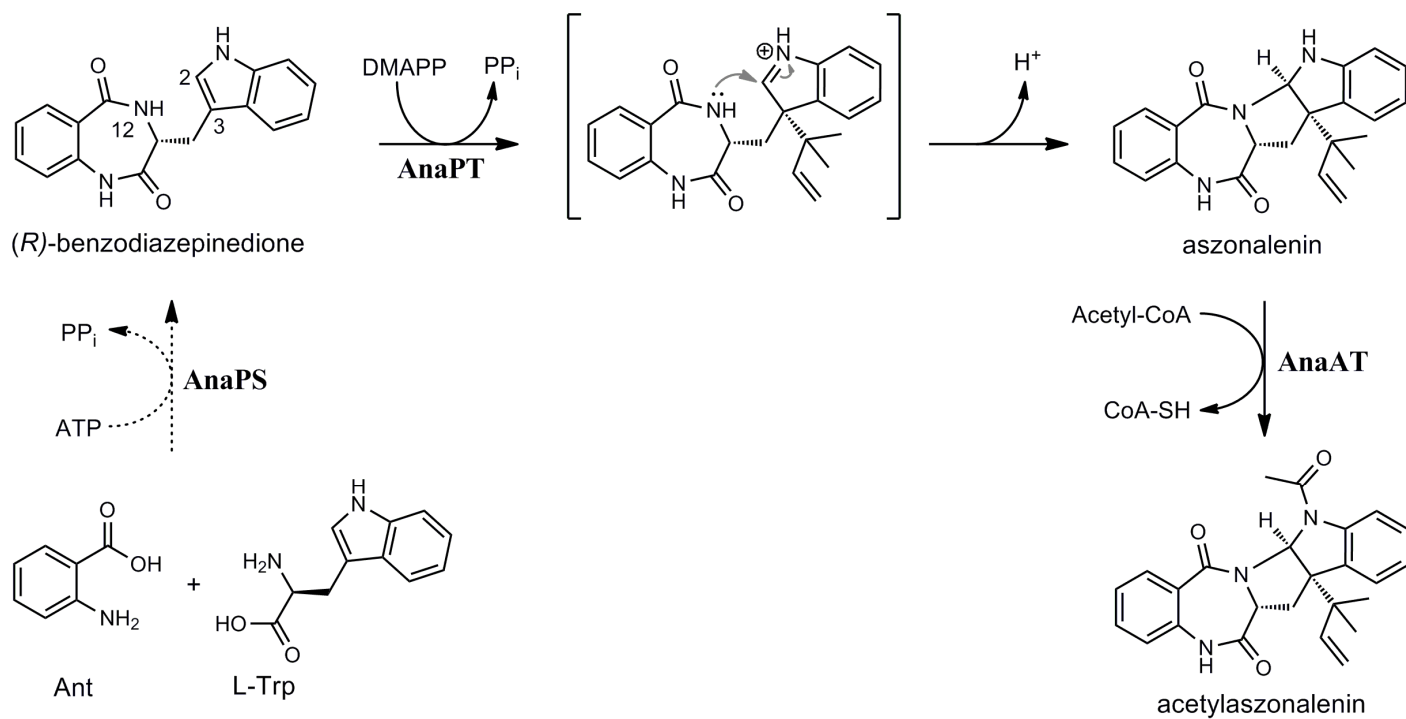


Figure S15. Proposed pathway for acetylaszonalenin biosynthesis, adapted from Wen-Bing Yin et al. (2).



References

1. Macheroux, P. (1999) UV-visible spectroscopy as a tool to study flavoproteins, In *Flavoprotein Protocols* (Chapman, S. K., and Reid, G. A., Eds.), pp 1-7, Humana Press.
2. Yin, W.-B., Grundmann, A., Cheng, J., and Li, S.-M. (2009) Acetylaszonalenin biosynthesis in *Neosartorya fischeri*: identification of the biosynthetic gene cluster by genomic mining and functional proof of the genes by biochemical investigation, *J. Biol. Chem.* 284, 100-109.